Electromagnetic neutrinos in laboratory experiments and astrophysics

Carlo Giunti[1], Konstantin A. Kouzakov[3], Yu-Feng Li[2], Alexey V. Lokhov[6], Alexander I. Studenikin[4,5,], and Shun Zhou[2]*

An overview of neutrino electromagnetic properties, which open a door to the new physics beyond the Standard Model, is given. The effects of neutrino electromagnetic interactions both in terrestrial experiments and in astrophysical environments are discussed. The experimental bounds on neutrino electromagnetic characteristics are summarized. Future astrophysical probes of electromagnetic neutrinos are outlined.

1 Introduction

The importance of neutrino electromagnetic properties was first mentioned by Pauli in 1930, when he postulated the existence of this particle and discussed the possibility that the neutrino might have a magnetic moment [1]. Systematic theoretical studies of neutrino electromagnetic properties started after it was shown that in the extended Standard Model with right-handed neutrinos the magnetic moment of a massive neutrino is, in general, nonvanishing and that its value is determined by the neutrino mass [2–8].

Neutrinos remained elusive until the detection of reactor neutrinos by Reines and Cowan around 1956 [9]. However, there was no sign of a neutrino mass. After the discovery of parity violation in 1957, the two-component theory of massless neutrinos was proposed [10–12], in which a neutrino is described by a Weyl spinor and there are only left-handed neutrinos and right-handed antineutrinos. It was however clear [13–15] that two-component neutrinos could be massive Majorana fermions and that the two-component theory of a massless neutrino is equivalent to the Majorana theory in the limit of zero neutrino mass.

The two-component theory of massless neutrinos was later incorporated in the Standard Model of Glashow, Weinberg and Salam [16–18], in which neutrinos are massless and have only weak interactions. In the Standard Model Majorana neutrino masses are forbidden by the $SU(2)_L \times U(1)_Y$ symmetry. We now know that neutrinos are massive, because many experiments observed neutrino oscillations (see the review articles [19–24]), which are generated by neutrino masses and mixing [25–28]. Therefore, the Standard Model must be extended to account for the neutrino masses. There are many possible extensions of the Standard Model which predict different properties for neutrinos (see [21, 29, 30]). Among them, most important is their fundamental Dirac or Majorana character. In many extensions of the Standard Model neutrinos acquire also electromagnetic properties through quantum loops' effects which allow interactions of neutrinos with electromagnetic fields and electromagnetic interactions of neutrinos with charged particles.

Hence, the theoretical and experimental study of neutrino electromagnetic interactions is a powerful tool in the search for a more fundamental theory beyond the Standard Model. Moreover, the electromagnetic interactions of neutrinos can generate important effects, especially in astrophysical environments, where neutrinos propagate over long distances in magnetic fields in vacuum and in matter. Unfortunately, in spite of many efforts in the search of neutrino electromagnetic interactions, up to now there is no positive experimental indication in favor

* Corresponding author E-mail: studenik@srd.sinp.msu.ru
1 INFN, Sezione di Torino, and Dipartimento di Fisica Teorica, Universit'a di Torino
2 Institite of High Energy Physics, Chinese Academy of Sciences, Beijing, China
3 Department of Nuclear Physics and Quantum Theory of Collisions, Faculty of Physics, Lomonosov Moscow State University, 119991 Moscow, Russia
4 Department of Theoretical Physics, Faculty of Physics, Lomonosov Moscow State University, 119991 Moscow, Russia
5 Joint Institute for Nuclear Research, 141980 Dubna, Moscow Region, Russia
6 Institute for Nuclear Research, Russian Academy of Sciences, 117312 Moscow, Russia

of their existence. However, it is expected that the Standard Model neutrino charge radii should be measured in the near future. This will be a test of the Standard Model and of the physics beyond the Standard Model which contributes to the neutrino charge radii. Moreover, the existence of neutrino masses and mixing implies that neutrinos have (diagonal and/or transition) magnetic moments. Since their values depend on the specific theory which extends the Standard Model in order to accommodate neutrino masses and mixing, experimentalists and theorists are eagerly looking for them.

The paper is organized as follows. Section 2 delivers the general form of the electromagnetic interactions of Dirac and Majorana neutrinos in the one-photon approximation, which are expressed in terms of electromagnetic form factors. In Section 3 we discuss some basic processes which are induced by the neutrino electromagnetic properties and some important effects due to the interaction of neutrinos with classical electromagnetic fields. In Section 4 we overview the experimental constraints on the neutrino electric and magnetic moments, the electric charge (millicharge), the charge radius and the anapole moment. In Section 5 future astrophysical probes of neutrino electromagnetic properties and interactions are outlined. Finally, Section 6 summarizes this work.

2 Neutrino electromagnetic characteristics

In this Section we discuss the general form of the electromagnetic interactions of Dirac and Majorana neutrinos in the one-photon approximation. In the Standard Model, the interaction of a fermionic field $\mathfrak{f}$ with the electromagnetic field A^μ is given by the interaction Hamiltonian

$$\mathscr{H}^{(\mathfrak{f})}_{\rm em} = j^{(\mathfrak{f})}_\mu A^\mu = e_\mathfrak{f} \bar{\mathfrak{f}} \gamma_\mu \mathfrak{f} A^\mu, \tag{1}$$

where $e_\mathfrak{f}$ is the charge of the fermion $\mathfrak{f}$.

For neutrinos the electric charge is zero and there are no electromagnetic interactions at tree-level[1]. At the same time, such interactions can arise at the quantum level from loop diagrams at higher order of the perturbative expansion of the interaction. We know that there are at least three massive neutrino fields in nature, which are mixed with the three active flavor neutrinos ν_e, ν_μ, ν_τ. Therefore, we discuss the case of three massive neutrino fields ν_i

[1] However, in some theories beyond the Standard Model neutrinos can be millicharged particles (see below).

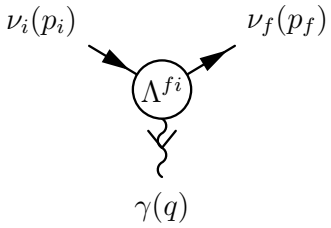

Figure 1 Effective one-photon coupling of neutrinos with the electromagnetic field, taking into account possible transitions between two different initial and final massive neutrinos ν_i and ν_f.

with respective masses m_i ($i = 1,2,3$). In the one-photon approximation, the effective electromagnetic interaction Hamiltonian is given by

$$\mathscr{H}^{(\nu)}_{\rm em} = j^{(\nu)}_\mu A^\mu = \sum_{i,f=1}^{3} \overline{\nu}_f \Lambda^{fi}_\mu \nu_i A^\mu, \tag{2}$$

where we take into account possible transitions between different massive neutrinos. The physical effect of $\mathscr{H}^{(\nu)}_{\rm em}$ is described by the effective electromagnetic vertex in Fig. 1. In momentum-space representation, this vertex depends only on the four-momentum $q = p_i - p_f$ transferred to the photon and can be expressed as follows:

$$\begin{aligned}\Lambda_\mu(q) = {} & \left(\gamma_\mu - q_\mu \not{q}/q^2\right)\left[f_Q(q^2) + f_A(q^2) q^2 \gamma_5\right] \\ & - i\sigma_{\mu\nu} q^\nu \left[f_M(q^2) + i f_E(q^2)\gamma_5\right],\end{aligned} \tag{3}$$

in which $\Lambda_\mu(q)$ is a 3×3 matrix in the space of massive neutrinos expressed in terms of the four Hermitian 3×3 matrices of form factors

$$f_Q = f_Q^\dagger, \qquad f_M = f_M^\dagger, \qquad f_E = f_E^\dagger, \qquad f_A = f_A^\dagger, \tag{4}$$

where Q, M, E, A refer respectively to the real charge, magnetic, electric, and anapole neutrino form factors. The Lorentz-invariant form of the vertex function (3) is also consistent with electromagnetic gauge invariance that implies four-current conservation.

For the coupling with a real photon in vacuum ($q^2 = 0$) we have

$$f_Q^{fi}(0) = e_{fi},\ f_M^{fi}(0) = \mu_{fi},\ f_E^{fi}(0) = \epsilon_{fi},\ f_A^{fi}(0) = a_{fi}, \tag{5}$$

where $e_{fi}, \mu_{fi}, \epsilon_{fi}$ and a_{fi} are, respectively, the neutrino charge, magnetic moment, electric moment and anapole moment of diagonal ($f = i$) and transition ($f \neq i$) types.

A Majorana neutrino is a neutral spin 1/2 particle which coincides with its antiparticle. The four degrees

of freedom of a Dirac field (two helicities and two particle-antiparticle) are reduced to two (two helicities). Since a Majorana field has half the degrees of freedom of a Dirac field, its electromagnetic properties are also reduced. Namely, in the Majorana case the charge, magnetic and electric form-factor matrices are antisymmetric and the anapole form-factor matrix is symmetric. Since $f_Q^{\rm M}$, $f_M^{\rm M}$ and $f_E^{\rm M}$ are antisymmetric, a Majorana neutrino does not have diagonal charge and dipole magnetic and electric form factors [13, 14, 31]. It can only have a diagonal anapole form factor. On the other hand, Majorana neutrinos can have as many off-diagonal (transition) form-factors as Dirac neutrinos.

Neutrino electric charge. It is usually believed that the neutrino electric charge $e_\nu = f_Q(0)$ is zero. This is often thought to be attributed to the gauge-invariance and anomaly-cancellation constraints imposed in the Standard Model. In the Standard Model of $\mathrm{SU}(2)_L \times \mathrm{U}(1)_Y$ electroweak interactions it is possible to get [32] a general proof that neutrinos are electrically neutral, which is based on the requirement of electric charges' quantization. The direct calculations of the neutrino charge in the Standard Model for massless (see, for instance [33, 34]) and massive neutrinos [35, 36] also prove that, at least at the one-loop level, the neutrino electric charge is gauge-independent and vanishes. However, if the neutrino has a mass, it still may become electrically millicharged. A brief discussion of different mechanisms for introducing millicharged particles including neutrinos can be found in [37]. In the case of millicharged massive neutrinos, electromagnetic gauge invariance implies that the diagonal electric charges e_{ii} $(i = 1, 2, 3)$ are equal[2]. It should be mentioned that the most stringent experimental constraints on the electric charge of the neutrino can be obtained from neutrality of matter. These and other constraints, including the astrophysical ones, are discussed in Section 4.

Neutrino charge radius. Even if the electric charge of a neutrino is zero, the electric form factor $f_Q(q^2)$ can still contain nontrivial information about neutrino static properties [38]. A neutral particle can be characterized by a superposition of two charge distributions of opposite signs, so that the particle form factor $f_Q(q^2)$ can be non-zero for $q^2 \neq 0$. The mean charge radius (in fact, it is the charged radius squared) of an electrically neutral neutrino is given by

$$\langle r_\nu^2 \rangle = 6 \left. \frac{d f_Q(q^2)}{d q^2} \right|_{q^2=0}, \qquad (6)$$

which is determined by the second term in the power-series expansion of the neutrino charge form factor.

Note that there is a long-standing discussion (see [38] for details) on the possibility to obtain for the neutrino charged radius a gauge-independent and finite quantity. In one of the first studies [33], it was claimed that in the Standard Model and in the unitary gauge the neutrino charge radius is ultraviolet-divergent and so it is not a physical quantity. However, it was shown [39] that in the unitary gauge it is possible to obtain for the neutrino charge radius a gauge-dependent but finite quantity. Later on, it was also shown [3] that considering additional box diagrams in combination with contributions from the proper diagrams it is possible to obtain a finite and gauge-independent value for the neutrino charge radius. In this way, the neutrino electroweak radius was defined in [40, 41] and an additional set of diagrams that give contribution to its value was discussed in [42]. Finally, in a series of papers [43–45] the neutrino electroweak radius as a physical observable has been introduced. This, however, revived the discussion [46–49] on the definition of the neutrino charge radius. Nevertheless, in the corresponding calculations, performed in the one-loop approximation including additional terms from the $\gamma - Z$ boson mixing and the box diagrams involving W and Z bosons, the following gauge-invariant result for the neutrino charge radius has been obtained [49]: $\langle r_{\nu_e}^2 \rangle = 4 \times 10^{-33}\ \mathrm{cm}^2$. This theoretical result differs at most by an order of magnitude from the available experimental bounds on $\langle r_\nu^2 \rangle$ (see Section 4 for references and more detailed discussion). Therefore, one may expect that the experimental accuracy will soon reach the level needed to probe the neutrino effective charge radius.

Neutrino electric and magnetic moments. The most well studied and understood among the neutrino electromagnetic characteristics are the dipole magnetic and electric moments, which are given by the corresponding form factors at $q^2 = 0$:

$$\mu_\nu = f_M(0), \qquad \epsilon_\nu = f_E(0). \qquad (7)$$

The diagonal magnetic and electric moments of a Dirac neutrino in the minimally-extended Standard Model with right-handed neutrinos, derived for the first time in [4], are respectively

$$\mu_{ii}^D = \frac{3 e_0 G_F m_i}{8\sqrt{2}\pi^2} \approx 3.2 \times 10^{-19} \mu_{\rm B} \left(\frac{m_i}{1\,\mathrm{eV}} \right), \qquad \epsilon_{ii}^D = 0, \qquad (8)$$

where $\mu_{\rm B}$ is the Bohr magneton. According to (8) the value of the neutrino magnetic moment is very small. However, in many other theoretical frameworks (beyond the minimally-extended Standard Model) the neutrino magnetic moment can reach values that are of interest for the

[2] The work is in preparation.

next generation of terrestrial experiments and also accessible for astrophysical observations. Note that the best laboratory upper limit on a neutrino magnetic moment, $\mu_\nu \leq 2.9 \times 10^{-11} \mu_B$ (90% CL), has been obtained by the GEMMA collaboration [50] (see Section 4), and the best astrophysical limit is $\mu_\nu \leq 3 \times 10^{-12} \mu_B$ (90% CL) [51]. The latter bound comes from the constraints on the possible delay of helium ignition of a red giant star in globular clusters due to the cooling induced by the energy loss in the plasmon-decay process $\gamma^* \to \nu\bar{\nu}$ (see Fig. 2(b)). Recently the limit has been updated in [52] using state-of-the-art astronomical observations and stellar evolution codes, with the results

$$\mu_\nu < \begin{cases} 2.6 \times 10^{-12} \mu_B & (68\% \text{ CL}), \\ 4.5 \times 10^{-12} \mu_B & (95\% \text{ CL}). \end{cases} \tag{9}$$

This astrophysical bound on a neutrino magnetic moment is applicable to both Dirac and Majorana neutrinos and constrains all diagonal and transition dipole moments.

Neutrino anapole moment. The notion of an anapole moment for a Dirac particle was introduced by Zeldovich [53] after the discovery of parity violation. In order to understand the physical characteristics of the anapole moment, it is useful to consider its effect in the interactions with external electromagnetic fields. The neutrino anapole moment contributes to the scattering of neutrinos with charged particles. In order to discuss its effects, it is convenient to consider strictly neutral neutrinos with $f_Q(0) = 0$ and define a reduced charge form factor $\tilde{f}_Q(q^2)$ such that

$$f_Q(q^2) = q^2 \, \tilde{f}_Q(q^2). \tag{10}$$

Then, from Eq. (6), apart from a factor 1/6, the reduced charge form factor at $q^2 = 0$ is just the squared neutrino charge radius:

$$\tilde{f}_Q(0) = \langle r_\nu^2 \rangle / 6. \tag{11}$$

Let us now consider the charge and anapole parts of the neutrino electromagnetic vertex function, as

$$\Lambda_\mu^{Q,A}(q) = \left(\gamma_\mu q^2 - q_\mu \not{q}\right) \left[\tilde{f}_Q(q^2) + f_A(q^2)\gamma_5\right]. \tag{12}$$

Since for ultrarelativistic neutrinos the effect of γ_5 is only a sign which depends on the helicity of the neutrino, the phenomenology of neutrino anapole moments is similar to that of neutrino charge radii. Hence, the limits on the neutrino charge radii discussed in Section 4 apply also to the neutrino anapole moments multiplied by a factor of 6.

3 Basic electromagnetic processes of neutrinos

Neutrino-electron elastic scattering. The most sensitive and widely used method for the experimental investigation of the neutrino magnetic moment is provided by direct laboratory measurements of low-energy elastic scattering of neutrinos and antineutrinos with electrons in reactor, accelerator and solar experiments[3]. Detailed descriptions of several experiments can be found in [58, 59].

Extensive experimental studies of the neutrino magnetic moment, performed during many years, are stimulated by the hope to observe a value much larger than the prediction in Eq. (8) of the minimally extended Standard Model with right-handed neutrinos. It would be a clear indication of new physics beyond the extended Standard Model. For example, the effective magnetic moment in $\bar{\nu}_e$-e elastic scattering in a class of extra-dimension models can be as large as about $10^{-10} \mu_B$ [60]. Future higher precision reactor experiments can therefore be used to provide new constraints on large extra-dimensions.

The possibility for neutrino-electron elastic scattering due to neutrino magnetic moment was first considered in [61] and the cross section of this process was calculated in [62] (for related short historical notes see [63]). Here we would like to recall the paper by Domogatsky and Nadezhin [64], where the cross section of [62] was corrected and the antineutrino-electron cross section was considered in the context of the earlier experiments with reactor antineutrinos of [65, 66], which were aimed to reveal the effects of the neutrino magnetic moment. Discussions on the derivation of the cross section and on the optimal conditions for bounding the neutrino magnetic moment, as well as a collection of cross section formulae for elastic scattering of neutrinos (antineutrinos) on electrons, nucleons, and nuclei can be found in [63, 67].

Let us consider the process

$$\nu_\ell + e^- \to \nu_{\ell'} + e^-, \tag{13}$$

where a neutrino or antineutrino with flavor $\ell = e, \mu, \tau$ and energy E_ν elastically scatters off a free electron (FE) at rest in the laboratory frame. Due to neutrino mixing, the final neutrino flavor ℓ' can be different from ℓ. There are two observables: the kinetic energy T_e of the recoil electron and the recoil angle χ with respect to the neutrino beam,

[3] The effects of a neutrino magnetic moment in other processes which can be observed in laboratory experiments have been discussed in [54–57].

which are related by

$$\cos\chi = \frac{E_\nu + m_e}{E_\nu}\left[\frac{T_e}{T_e + 2m_e}\right]^{1/2}. \tag{14}$$

The electron kinetic energy is constrained from the energy-momentum conservation by

$$T_e \leq \frac{2E_\nu^2}{2E_\nu + m_e}. \tag{15}$$

Since, in the ultrarelativistic limit, the neutrino magnetic moment interaction changes the neutrino helicity and the Standard Model weak interaction conserves the neutrino helicity, the two contributions add incoherently in the cross section[4] which can be written as [67],

$$\frac{d\sigma_{\nu_\ell e^-}}{dT_e} = \left(\frac{d\sigma_{\nu_\ell e^-}}{dT_e}\right)^{\rm FE}_{\rm SM} + \left(\frac{d\sigma_{\nu_\ell e^-}}{dT_e}\right)^{\rm FE}_{\rm mag}. \tag{16}$$

The weak-interaction cross section is given by

$$\begin{aligned}\left(\frac{d\sigma_{\nu_\ell e^-}}{dT_e}\right)^{\rm FE}_{\rm SM} = \frac{G_F^2 m_e}{2\pi}\Big\{&(g_V^{\nu_\ell} + g_A^{\nu_\ell})^2 \\ &+ (g_V^{\nu_\ell} - g_A^{\nu_\ell})^2\left(1 - \frac{T_e}{E_\nu}\right)^2 \\ &+ \left[(g_A^{\nu_\ell})^2 - (g_V^{\nu_\ell})^2\right]\frac{m_e T_e}{E_\nu^2}\Big\},\end{aligned} \tag{17}$$

with the standard coupling constants g_V and g_A given by

$$g_V^{\nu_e} = 2\sin^2\theta_W + 1/2, \qquad g_A^{\nu_e} = 1/2, \tag{18}$$

$$g_V^{\nu_{\mu,\tau}} = 2\sin^2\theta_W - 1/2, \qquad g_A^{\nu_{\mu,\tau}} = -1/2. \tag{19}$$

For antineutrinos one must substitute $g_A \to -g_A$.

The neutrino magnetic-moment contribution to the cross section is given by [67]

$$\left(\frac{d\sigma_{\nu_\ell e^-}}{dT_e}\right)^{\rm FE}_{\rm mag} = \frac{\pi\alpha^2}{m_e^2}\left(\frac{1}{T_e} - \frac{1}{E_\nu}\right)\left(\frac{\mu_{\nu_\ell}}{\mu_{\rm B}}\right)^2, \tag{20}$$

where μ_{ν_ℓ} is the effective magnetic moment discussed in the following Section. It is called traditionally "magnetic moment", but it receives contributions from both the electric and magnetic dipole moments (see details in Section 4).

The two terms $(d\sigma_{\nu_\ell e^-}/dT_e)^{\rm FE}_{\rm SM}$ and $(d\sigma_{\nu_\ell e^-}/dT_e)^{\rm FE}_{\rm mag}$ exhibit quite different dependencies on the experimentally observable electron kinetic energy T_e. One can see that small values of the neutrino magnetic moment can be probed by lowering the electron recoil energy threshold. In fact, considering $T_e \ll E_\nu$ in Eq. (20) and neglecting the coefficients due to $g_V^{\nu_\ell}$ and $g_A^{\nu_\ell}$ in Eq. (17), one can find that $(d\sigma/dT_e)^{\rm FE}_{\rm mag}$ exceeds $(d\sigma/dT_e)^{\rm FE}_{\rm SM}$ for

$$T_e \lesssim \frac{\pi^2\alpha^2}{G_{\rm F}^2 m_e^3}\left(\frac{\mu_\nu}{\mu_{\rm B}}\right)^2. \tag{21}$$

The current experiments with reactor antineutrinos have reached threshold values of T_e as low as few keV. As discussed in Section 6, these experiments are likely to further improve the sensitivity to low energy deposition in the detector. At low energies however one can expect a modification of the free-electron formulas (17) and (20) due to the binding of electrons in the germanium atoms, where e.g. the energy of the K_α line, 9.89 keV, indicates that at least some of the atomic binding energies are comparable to the already relevant to the experiment values of T_e. It was demonstrated [69–73] by means of analytical and numerical calculations that the atomic binding effects are adequately described by the so-called stepping approximation introduced in [74] from interpretation of numerical data. According to the stepping approach,

$$\left(\frac{d\sigma_{\nu_\ell e^-}}{dT_e}\right)_{\rm SM} = \left(\frac{d\sigma_{\nu_\ell e^-}}{dT_e}\right)^{\rm FE}_{\rm SM}\sum_j n_j\theta(T_e - E_j), \tag{22}$$

$$\left(\frac{d\sigma_{\nu_\ell e^-}}{dT_e}\right)_{\rm mag} = \left(\frac{d\sigma_{\nu_\ell e^-}}{dT_e}\right)^{\rm FE}_{\rm mag}\sum_j n_j\theta(T_e - E_j), \tag{23}$$

where the j sum runs over all occupied atomic sublevels, with n_j and E_j being their occupations and binding energies.

Neutrino-nucleus coherent scattering. As mentioned above, the most sensitive probe of neutrino electromagnetic properties is provided by direct laboratory measurements of (anti)neutrino-electron scattering at low energies in solar, accelerator and reactor experiments (their detailed description can be found in [38, 58, 59, 75–77]). The coherent elastic neutrino-nucleus scattering [78] has not been experimentally observed so far, but it is expected to be accessible in the reactor experiments when lowering the energy threshold of the employed Ge detectors [79–81].

Let us consider the case of electron neutrino scattering off a spin-zero nucleus with even numbers of protons and neutrons, Z and N. The matrix element of this process, taking into account the neutrino electromagnetic

[4] The small interference term due to neutrino masses has been derived in [68].

properties, reads

$$\mathcal{M} = \left[\frac{G_F}{\sqrt{2}} \bar{u}(k')\gamma^\mu(1-\gamma_5)u(k)C_V + \frac{4\pi Ze}{q^2}\left(e_{\nu_e} + \frac{e}{6}q^2\langle r^2_{\nu_e}\rangle\right)\bar{u}(k')\gamma^\mu u(k) - \frac{4\pi Ze\mu_{\nu_e}}{q^2}\bar{u}(k')\sigma^{\mu\nu}q_\nu u(k)\right] j^{(N)}_\mu, \quad (24)$$

where $C_V = [Z(1-4\sin^2\theta_W)-N]/2$, $j^{(N)}_\mu = (p_\mu + p'_\mu)F(q^2)$, with p and p' being the initial and final nuclear four-momenta. For neutrinos with energies of a few MeV the maximum momentum transfer squared ($|q^2|_{\max} = 4E^2_\nu$) is still small compared to $1/R^2$, where R, the nucleus radius, is of the order of $10^{-2} - 10^{-1}$ MeV^{-1}. Therefore, the nuclear elastic form factor $F(q^2)$ can be set equal to one. Using (24), one obtains the differential cross section in the nuclear-recoil energy transfer T_N as a sum of two components. The first component conserves the neutrino helicity and can be presented in the form

$$\left(\frac{d\sigma_{\nu_e N}}{dT_N}\right)^Q_{\rm SM} = \eta^2 \left(\frac{d\sigma_{\nu_e N}}{dT_N}\right)_{\rm SM}, \quad (25)$$

where

$$\eta = 1 - \frac{\sqrt{2}\pi eZ}{G_F C_V}\left[\frac{e_{\nu_e}}{MT} - \frac{e}{3}\langle r^2_{\nu_e}\rangle\right],$$

with M being the nuclear mass, and

$$\left(\frac{d\sigma_{\nu_e N}}{dT_N}\right)_{\rm SM} = \frac{G^2_F}{\pi} M C^2_V \left(1 - \frac{T_N}{T^{\max}_N}\right) \quad (26)$$

is the Standard Model cross section due to weak interaction [82], with

$$T^{\max}_N = \frac{2E^2_\nu}{2E_\nu + M}.$$

The second, helicity-flipping component is due to the magnetic moment only and is given by [67]

$$\left(\frac{d\sigma_{\nu_e N}}{dT_N}\right)_{\rm mag} = 4\pi\alpha\mu^2_{\nu_e}\frac{Z^2}{T_N}\left(1 - \frac{T_N}{E_\nu} + \frac{T^2_N}{4E^2_\nu}\right). \quad (27)$$

Clearly, any deviation of the measured cross section of the process under discussion from the well-known Standard Model value (26) will provide a signature of the physics beyond the Standard Model (see also [83–86]). Formulas (25) and (27) describe such a deviation due to neutrino electromagnetic interactions.

Radiative decay and related processes. The magnetic and electric (transition) dipole moments of neutrinos, as well as possible very small electric charges (millicharges), describe direct couplings of neutrinos with photons

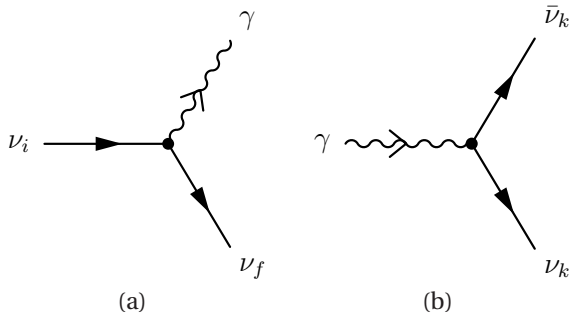

Figure 2 Feynman diagrams for neutrino radiative decay and Cherenkov radiation (a) and plasmon decay (b). The depicted electromagnetic interaction vertices are supposed to be effective (such as the one-photon coupling in Fig. 1).

which induce several observable decay processes. In this Section we discuss the decay processes generated by the diagrams in Fig. 2: the diagram in Fig. 2(a) generates neutrino radiative decay $\nu_i \to \nu_f + \gamma$ and the processes of neutrino Cherenkov radiation and spin light ($SL\nu$) of a neutrino propagating in a medium; the diagram in Fig. 2(b) generates photon (plasmon) decay to an neutrino-antineutrino pair in a plasma ($\gamma^* \to \nu\bar{\nu}$).

If the masses of neutrinos are nondegenerate, the radiative decay of a heavier neutrino ν_i into a lighter neutrino ν_f (with $m_i > m_f$) with emission of a photon,

$$\nu_i \to \nu_f + \gamma, \quad (28)$$

may proceed in vacuum [2,3,5–7,87–89]. Early discussions of the possible role of neutrino radiative decay in different astrophysical and cosmological settings can be found in [90–95]. The first estimates for the process of massive neutrino decay were presented in [89]. They considered various processes of neutrino decay, for instance, the decay into three neutrinos $\nu \to \nu + \nu + \bar{\nu}$ and the radiative decay $\nu_1 \to \nu_2 + \gamma$.

In [95] the possible existence of relic slow massive neutrinos was considered. The radiative decay of the neutrino into an ultraviolet photon and a light neutrino becomes then an indicator of these relic particles. The first one-loop calculation of the neutrino radiative decay was performed in [5,6] and yielded the decay rate as

$$\Gamma = \frac{\alpha G^2_F}{128\pi^4}\left(\frac{m^2_1 - m^2_2}{m_1}\right)^3 (m^2_1 + m^2_2)\left|\sum_{\ell=e,\mu,\tau} U^*_{\ell 1} U_{\ell 2} r_\ell\right|^2, \quad (29)$$

where $r_\ell \simeq 3(m_\ell/2m_W)^2$ ($\ell = e,\mu,\tau$), m_W is the mass of W-boson, and $U_{\ell i}$ are the mixing-matrix elements.

The rate of neutrino radiative decay in relativistic and non-relativistic media consisting of electrons (without muons and taus) was calculated in Ref. [96] in the framework of finite-temperature quantum field theory. The presence of the medium prevents the Glashow-Iliopoulos-Maiani [97] suppression of the decay, which is strongly enhanced in high-density matter (neutron star, supernova, etc.). In Ref. [98] the influence of dissipation and dispersion in the medium, that can be important for the phenomenological studies of the early Universe, was taken into account. As shown in Ref. [99], one can also calculate the rate of neutrino radiative decay in matter avoiding the formalism of finite-temperature field theory by considering the effective averaged interaction with the medium.

Spin light of neutrino in matter. The recent studies of neutrino electromagnetic properties revealed a new mechanism of electromagnetic radiation by a neutrino propagating in dense matter that has been proposed in [100]. This type of electromagnetic radiation was called the spin light of neutrino in matter (*SLν*). In a quasi-classical treatment this radiation is due to neutrino magnetic moment precession in dense background matter. The quantum theory of this phenomena has been developed in [101–103].

The *SLν* is a process of photon emission in neutrino transition between different helicity states in matter. As it has been shown in Ref. [101,103], in the relativistic regime the *SLν* mechanism could provide up to one half of the initial neutrino energy transition to the emitted radiation. It was also shown that the *SLν* provides the spin polarization effect of neutrino beam moving in matter (similarly to the well-known effect of the electron spin self-polarization in synchrotron radiation [104]).

The characteristics of the *SLν* depend on the components of the medium. The *SLν* is radiated by a neutrino with negative helicity while propagating in matter consisting of electrons. In the medium consisting of neutrons the *SLν* is produced by an antineutrino with positive helicity.

For the relativistic neutrinos the radiation is focused into a narrow cone in the direction of the initial neutrino. The radiation of ultra-relativistic neutrinos in matter has circular polarization which in some cases (high density) reaches 100%. The average energy of the radiated photons depends on the energy of the initial neutrinos and in dense medium reaches one half of the initial neutrino energy (see also [105, 106]).

Along with studying the conventional spin light of neutrino in matter with the mass for the initial and final neutrino states one can consider the spin light process in neutrino transition between different mass states with masses m_1 and m_2, $m_1 > m_2$. The emitted photon is coupled to the neutrinos by the transition magnetic moment μ_{fi}. To avoid cumbersome formulae, the effects of oscillations were neglected and the matter with only a neutron component was considered ($n_n \gg n_e \approx n_p$). It was shown [107, 108] that the rate of *SLν* in the neutrino radiative decay acquires additional terms that are proportional to the difference of the initial and final neutrino masses squared: $\delta = \frac{m_1^2 - m_2^2}{p_1^2}$. As opposed to the *SLν* with the same mass of the initial and final state, the process is kinematically open for the quasi-vacuum case, when the density of the background medium is small. In addition, the expression for the rate of the process can be reduced to the results of previous neutrino radiative decay calculations. The influence of external fields and matter on a massive neutrino decay was further considered in [109]

Neutrino interaction with electromagnetic fields. If neutrinos have nontrivial electromagnetic properties, they can interact with classical electromagnetic fields. Significant effects can occur, in particular, in neutrino astrophysics, since neutrinos can propagate over very long distances in astrophysical environments with magnetic fields. In this case even a very weak interaction can have large cumulative effects.

A classical electromagnetic field produces spin and spin-flavor neutrino transitions [4, 110–114]. This kind of interaction can yield observable effects, for instance, in the solar neutrino data [115–122]. The neutrino effective magnetic moment is also modified in very strong external magnetic fields [123]. It has been recently shown that due to the nontrivial electromagnetic properties the production of neutrino-antineutrino pairs becomes possible in very strong magnetic fields [124]. It can be also important to account for the external electromagnetic fields and for the background matter simultaneously. In various astrophysical situations the effects of fields and matter can either cancel or enhance each other.

For instance, an approach based on the generalized Bargmann-Michel-Telegdi equation can be used for derivation of an impact of matter motion and polarization on the neutrino spin (and spin-flavor) evolution. Consider, as an example, an electron neutrino spin precession in the case when neutrinos with the Standard Model interaction are propagating through moving and polarized matter composed of electrons (electron gas) in the presence of an electromagnetic field given by the electromagnetic-field tensor $F_{\mu\nu} = (\vec{E}, \vec{B})$. As discussed in [125] (see also [126, 127]) the evolution of the three-dimensional neutrino spin vector $\vec{S}$ is given by

$$\frac{d\vec{S}}{dt} = \frac{2\mu}{\gamma}\left[\vec{S} \times (\vec{B}_0 + \vec{M}_0)\right], \tag{30}$$

where the magnetic field $\overrightarrow{B_0}$ in the neutrino rest frame is determined by the transversal and longitudinal (with respect to the neutrino motion) magnetic and electric field components in the laboratory frame,

$$\vec{B}_0 = \gamma\Big(\vec{B}_\perp + \frac{1}{\gamma}\vec{B}_\parallel + \sqrt{1-\gamma^{-2}}\Big[\vec{E}_\perp \times \frac{\vec{\beta}}{\beta}\Big]\Big). \tag{31}$$

The matter term $\vec{M}_0$ in Eq. (30) is also composed of the transversal $\vec{M}_{0_\parallel}$ and longitudinal $\overrightarrow{M_{0_\perp}}$ parts,

$$\overrightarrow{M_0} = \vec{M}_{0_\parallel} + \overrightarrow{M_{0_\perp}}, \tag{32}$$

$$\begin{aligned}\vec{M}_{0_\parallel} = \gamma\vec{\beta}\frac{n_0}{\sqrt{1-v_e^2}}\Bigg\{\rho_e^{(1)}\left(1-\frac{\vec{v}_e\vec{\beta}}{1-\gamma^{-2}}\right)\\ -\rho_e^{(2)}\left(\vec{\zeta}_e\vec{\beta}\sqrt{1-v_e^2}+\frac{(\vec{\zeta}_e\vec{v}_e)(\vec{\beta}\vec{v}_e)}{1+\sqrt{1-v_e^2}}\right)\frac{1}{1-\gamma^{-2}}\Bigg\},\end{aligned} \tag{33}$$

$$\begin{aligned}\vec{M}_{0_\perp} = -\frac{n_0}{\sqrt{1-v_e^2}}\Bigg\{\vec{v}_{e_\perp}\Big(\rho_e^{(1)}+\rho_e^{(2)}\frac{(\vec{\zeta}_e\vec{v}_e)}{1+\sqrt{1-v_e^2}}\Big)\\ +\vec{\zeta}_{e_\perp}\rho_e^{(2)}\sqrt{1-v_e^2}\Bigg\}.\end{aligned} \tag{34}$$

Here $n_0 = n_e\sqrt{1-v_e^2}$ is the invariant number density of matter given in the reference frame for which the total speed of matter is zero. The vectors $\vec{v}_e$, and $\vec{\zeta}_e$ ($0 \leqslant |\vec{\zeta}_e|^2 \leqslant 1$) denote, respectively, the speed of the reference frame in which the mean momentum of matter (electrons) is zero, and the mean value of the polarization vector of the background electrons in the above mentioned reference frame. The coefficients $\rho_e^{(1,2)}$ are calculated if the neutrino Lagrangian is given, and within the extended Standard Model supplied with $SU(2)$-singlet right-handed neutrino ν_R,

$$\rho_e^{(1)} = \frac{\tilde{G}_F}{2\sqrt{2}\mu}, \qquad \rho_e^{(2)} = -\frac{G_F}{2\sqrt{2}\mu}, \tag{35}$$

where $\tilde{G}_F = G_F(1+4\sin^2\theta_W)$. For the probability of the neutrino spin oscillations in the adiabatic approximation we get from Eqs. (33) and (34)

$$P_{\nu_L\to\nu_R}(x) = \sin^2 2\theta_{\rm eff}\sin^2\frac{\pi x}{L_{\rm eff}}, \tag{36}$$

$$\sin^2 2\theta_{\rm eff} = \frac{E_{\rm eff}^2}{E_{\rm eff}^2+\Delta_{\rm eff}^2}, \quad L_{\rm eff} = \frac{2\pi}{\sqrt{E_{\rm eff}^2+\Delta_{\rm eff}^2}}, \tag{37}$$

where

$$E_{\rm eff} = \mu\Big|\vec{B}_\perp + \frac{1}{\gamma}\vec{M}_{0\perp}\Big|, \tag{38}$$

$$\Delta_{\rm eff}^2 = \frac{\mu}{\gamma}\Big|\vec{M}_{0\parallel} + \vec{B}_{0\parallel}\Big|. \tag{39}$$

It follows that even without presence of an electromagnetic field, $\vec{B}_\perp = \vec{B}_{0\parallel} = 0$, neutrino spin (or spin-flavor) oscillations can be induced in the presence of matter when the transverse matter term $\vec{M}_{0\perp}$ is not zero. This possibility is realized in the case of nonzero transversal matter velocity or polarization. A detailed discussion of this phenomenon can be found in [125, 128].

4 Experimental limits on neutrino electromagnetic properties

Effective magnetic moment. In scattering experiments the neutrino is created at some distance from the detector as a flavor neutrino, which is a superposition of massive neutrinos. Therefore, the magnetic moment that is measured in these experiments is not that of a single massive neutrino, but it is an effective magnetic moment which takes into account neutrino mixing and the oscillations during the propagation between source and detector [68, 129]. In the following, when we refer to an effective magnetic moment of a flavor neutrino without indication of a source-detector distance L it is implicitly understood that L is small, such that the effective magnetic moment is independent of the neutrino energy and from the source-detector distance. In such a case, the effective magnetic moment is given by [38]

$$\mu_{\nu_\ell}^2 \simeq \mu_{\bar{\nu}_\ell}^2 \simeq \sum_{f=1}^{3}\left|\sum_{i=1}^{3}U_{\ell i}^*\left(\mu_{fi}-i\epsilon_{fi}\right)\right|^2. \tag{40}$$

Another situation where the effective magnetic moment does not depend on the neutrino energy and on the source-detector distance is when the source-detector distance is much larger than all the oscillation lengths $L_{fi} = 4\pi E_\nu/|\Delta m_{fi}^2|$. The effective magnetic moment in this case is evaluated as [38]

$$\mu_{\nu_\ell}^2 \simeq \mu_{\bar{\nu}_\ell}^2 \simeq \sum_{i=1}^{3}|U_{\ell i}|^2\sum_{f=1}^{3}\left|\mu_{fi}-i\epsilon_{fi}\right|^2. \tag{41}$$

Note that in the case of solar neutrinos, which have been used by the Super-Kamiokande [130] and Borexino [131] experiments to search for neutrino magnetic moments,

one must take into account the matter effects. The latter can be done by replacing the neutrino mixing matrix in Eq. (41) with the effective mixing matrix in matter at the point of neutrino production inside the Sun (see [38] and references therein).

It is also interesting to note that flavor neutrinos can have effective magnetic moments even if massive neutrinos are Majorana particles. In this case, since massive Majorana neutrinos do not have diagonal magnetic and electric dipole moments, the effective magnetic moments of flavor neutrinos receive contributions only from the transition dipole moments.

The constraints on the neutrino magnetic moments in direct laboratory experiments have been obtained so far from the lack of any observable distortion of the recoil electron energy spectrum. Experiments of this type have started in the 50's at the Savannah River Laboratory where the $\bar{\nu}_e$-e^- elastic scattering process was studied [65, 66, 140] with somewhat controversial results, as discussed by [67]. The most significant experimental limits on the effective magnetic moment μ_{ν_e} which have been obtained in measurements of reactor $\bar{\nu}_e$-e^- elastic scattering after about 1990 are listed in Tab. 1 (some details of the different experimental setups are reviewed in [77]).

An attempt to improve the experimental bound on μ_{ν_e} in reactor experiments was undertaken in [141], where it was suggested that in $\bar{\nu}_e$ interactions on an atomic target the atomic electron binding ("atomic-ionization effect") can significantly increase the electromagnetic contribution to the differential cross section with respect to the free-electron approximation. However, the dipole approximation used to derive the atomic-ionization effect is not valid for the electron antineutrino cross section in reactor neutrino magnetic moment experiments. Instead, the free electron approximation is appropriate for the interpretation of the data of reactor neutrino experiments and the current constraints in Tab. 1 cannot be improved by considering the atomic electron binding [69–73, 142, 143]. The history and present status of the theory of neutrino-atom collisions is reviewed in [144].

The current best limit on μ_{ν_e} has been obtained in 2012 in the GEMMA experiment at the Kalinin Nuclear Power Plant (Russia) with a 1.5 kg highly pure germanium detector exposed at a $\bar{\nu}_e$ flux of $2.7 \times 10^{13}\,\mathrm{cm^{-2}\,s^{-1}}$ at a distance of 13.9 m from the core of a $3\,\mathrm{GW_{th}}$ commercial water-moderated reactor [50]. The competitive TEXONO experiment is based at the Kuo-Sheng Reactor Neutrino Laboratory (Taiwan), where a 1.06 kg highly pure germanium detector was exposed to the flux of $\bar{\nu}_e$ at a distance of 28 m from the core of a $2.9\,\mathrm{GW_{th}}$ commercial reactor [135][5].

Searches for effects of neutrino magnetic moments have been performed also in accelerator experiments. The LAMPF bounds on μ_{ν_e} in Tab. 1 have been obtained with ν_e from μ^+ decay [136]. The LAMPF and LSND bounds on μ_{ν_μ} in Tab. 1 have been obtained with ν_μ and $\bar{\nu}_\mu$ from π^+ and μ^+ decay [136, 138]. The DONUT collaboration [139] investigated ν_τ-e^- and $\bar{\nu}_\tau$-e^- elastic scattering, finding the limit on μ_{ν_τ} in Tab. 1.

Solar neutrino experiments can also search for a neutrino magnetic moment signal by studying the shape of the electron spectrum [129]. Table 1 gives the limits obtained in the Super-Kamiokande experiment [130] for

$$\mu_{\rm S}^2(E_\nu \gtrsim 5\,\mathrm{MeV}) \simeq \cos^2\vartheta_{13} \sum_{i=1}^{3} \left|\mu_{i2} - i\epsilon_{i2}\right|^2 + \sin^2\vartheta_{13} \sum_{i=1}^{3} \left|\mu_{i3} - i\epsilon_{i3}\right|^2 , \quad (42)$$

where ϑ_{13} is the mixing angle, and that obtained in the Borexino experiment [131] for

$$\mu_{\rm S}(E_\nu \lesssim 1\,\mathrm{MeV}) \simeq \mu_{\nu_e}, \quad (43)$$

where μ_{ν_e} is given by Eq. (41).

Information on neutrino magnetic moments has been obtained also with global fits of solar neutrino data [147–149]. Considering Majorana three-neutrino mixing, the authors of [149] obtained, at 90% CL,

$$\sqrt{|\mu_{12}|^2 + |\mu_{23}|^2 + |\mu_{31}|^2} < 4.0 \times 10^{-10}\,\mu_{\rm B}, \quad (44)$$

from the analysis of solar and KamLAND, and

$$\sqrt{|\mu_{12}|^2 + |\mu_{23}|^2 + |\mu_{31}|^2} < 1.8 \times 10^{-10}\,\mu_{\rm B}, \quad (45)$$

adding the Rovno [133], TEXONO [150] and MUNU [151] constraints.

The neutrino magnetic moment contribution to the (anti)neutrino-electron elastic scattering process flips the neutrino helicity. If neutrinos are Dirac particles, this process transforms active left-handed neutrinos into sterile right-handed neutrinos, leading to dramatic effects on the explosion of a core-collapse supernova [152–161], where there are also contributions from the (anti)neutrino-proton and (anti)neutrino-neutron elastic scattering. Requiring that the entire energy in a supernova collapse

[5] The TEXONO and GEMMA data have been also used by [145, 146] to constrain neutrino nonstandard interactions.

Method	Experiment	Limit	CL	Reference
Reactor $\bar{\nu}_e$-e^-	Krasnoyarsk	$\mu_{\nu_e} < 2.4 \times 10^{-10}\,\mu_B$	90%	[132]
	Rovno	$\mu_{\nu_e} < 1.9 \times 10^{-10}\,\mu_B$	95%	[133]
	MUNU	$\mu_{\nu_e} < 9 \times 10^{-11}\,\mu_B$	90%	[134]
	TEXONO	$\mu_{\nu_e} < 7.4 \times 10^{-11}\,\mu_B$	90%	[135]
	GEMMA	$\mu_{\nu_e} < 2.9 \times 10^{-11}\,\mu_B$	90%	[50]
Accelerator ν_e-e^-	LAMPF	$\mu_{\nu_e} < 1.1 \times 10^{-9}\,\mu_B$	90%	[136]
Accelerator $(\nu_\mu, \bar{\nu}_\mu)$-e^-	BNL-E734	$\mu_{\nu_\mu} < 8.5 \times 10^{-10}\,\mu_B$	90%	[137]
	LAMPF	$\mu_{\nu_\mu} < 7.4 \times 10^{-10}\,\mu_B$	90%	[136]
	LSND	$\mu_{\nu_\mu} < 6.8 \times 10^{-10}\,\mu_B$	90%	[138]
Accelerator $(\nu_\tau, \bar{\nu}_\tau)$-$e^-$	DONUT	$\mu_{\nu_\tau} < 3.9 \times 10^{-7}\,\mu_B$	90%	[139]
Solar ν_e-e^-	Super-Kamiokande	$\mu_S(E_\nu \gtrsim 5\,\text{MeV}) < 1.1 \times 10^{-10}\,\mu_B$	90%	[130]
	Borexino	$\mu_S(E_\nu \lesssim 1\,\text{MeV}) < 5.4 \times 10^{-11}\,\mu_B$	90%	[131]

Table 1 Experimental limits for different neutrino effective magnetic moments.

is not carried away by the escaping sterile right-handed neutrinos created in the supernova core, the authors of [159, 160] obtained the following upper limit on a generic neutrino magnetic moment:

$$\mu_\nu \lesssim (0.1 - 0.4) \times 10^{-11}\,\mu_B, \tag{46}$$

which is slightly more stringent than the bound $\mu_\nu \lesssim (0.2 - 0.8) \times 10^{-11}\,\mu_B$ obtained in [156].

There is a gap of many orders of magnitude between the present experimental limits on neutrino magnetic moments of the order of $10^{-11}\,\mu_B$ and the prediction smaller than about $10^{-19}\,\mu_B$ in Eq. (8) of the minimal extension of the Standard Model with right-handed neutrinos. The hope to reach in the near future an experimental sensitivity of this order of magnitude is very small, taking into account that the experimental sensitivity of reactor $\bar{\nu}_e$-e elastic scattering experiments has improved by only one order of magnitude during a period of about twenty years (see [67], where a sensitivity of the order of $10^{-10}\,\mu_B$ is discussed). However, the experimental studies of neutrino magnetic moments are stimulated by the hope that new physics beyond the minimally extended Standard Model with right-handed neutrinos might give much stronger contributions.

Neutrino millicharge. The most severe experimental constraint on neutrino electric charges is that on the effective electron neutrino charge e_{ν_e}, which can be obtained from electric charge conservation in neutron beta decay $n \to p + e^- + \bar{\nu}_e$, from the experimental limits on the non-neutrality of matter which constrain the sum of the proton and electron charges, $e_p + e_e$, and from the experimental limits on the neutron charge e_n [162, 163]. Several experiments which measured the neutrality of matter give their results in terms of

$$e_{\text{mat}} = \frac{Z(e_p + e_e) + N e_n}{A}, \tag{47}$$

where $A = Z + N$ is the atomic mass of the substance under study, Z is its atomic number and N is its neutron number. From electric charge conservation in neutron beta decay, we have

$$e_{\nu_e} = e_n - (e_p + e_e) = \frac{A}{Z}\,(e_n - e_{\text{mat}})\,. \tag{48}$$

The best recent bound on the non-neutrality of matter [164],

$$e_{\text{mat}} = (-0.1 \pm 1.1) \times 10^{-21}\,e, \tag{49}$$

has been obtained with SF_6, which has $A = 146.06$ and $Z = 70$. Using the independent measurement of the charge of the free neutron [165]

$$e_n = (-0.4 \pm 1.1) \times 10^{-21}\,e, \tag{50}$$

we obtain

$$e_{\nu_e} = (-0.6 \pm 3.2) \times 10^{-21}\,e. \tag{51}$$

This value is compatible with the neutrality of matter limit in Tab. 2, which has been derived [162, 163] from the value of e_n in Eq. (50) and $e_{\text{mat}} = (0.8 \pm 0.8) \times 10^{-21}\,e$ [166].

It is also interesting that the effective charge of $\bar{\nu}_e$ can be constrained by the SN 1987A neutrino measurements taking into account that galactic and extragalactic magnetic field can lengthen the path of millicharged neutrinos and requiring that neutrinos with different energies arrive on Earth within the observed time interval of a few seconds [167]:

$$|e_{\nu_e}| \lesssim 3.8 \times 10^{-12} \frac{(E_\nu/10\,\mathrm{MeV})}{(d/10\,\mathrm{kpc})(B/1\,\mu\mathrm{G})} \sqrt{\frac{\Delta t/t}{\Delta E_\nu/E_\nu}}, \tag{52}$$

considering a magnetic field B acting over a distance d and the corresponding time $t = d/c$. $E_\nu \approx 15\,\mathrm{MeV}$ is the average neutrino energy, $\Delta E_\nu \approx E_\nu/2$ is the energy spread, and $\Delta t \approx 5\,\mathrm{s}$ is the arrival time interval. The authors of [167] considered two cases:

1. An intergalactic field $B \approx 10^{-3}\,\mu\mathrm{G}$ acting over the whole path $d \simeq 50\,\mathrm{kpc}$, which corresponds to $t \simeq 5 \times 10^{12}\,\mathrm{s}$, gives
$$|e_{\nu_e}| \lesssim 2 \times 10^{-15}\, e. \tag{53}$$
2. A galactic field $B \approx 1\,\mu\mathrm{G}$ acting over a distance $d \simeq 10\,\mathrm{kpc}$, which corresponds to $t \simeq 1 \times 10^{12}\,\mathrm{s}$, gives
$$|e_{\nu_e}| \lesssim 2 \times 10^{-17}\, e. \tag{54}$$

The last two limits in Tab. 2 have been obtained [170, 171] considering the results of reactor neutrino magnetic moment experiments. The differential cross section of the $\bar{\nu}_e$–e^- elastic scattering process due to a neutrino effective charge e_{ν_e} is given by (see [172])

$$\left(\frac{d\sigma}{dT_e}\right)_{\mathrm{charge}} \simeq 2\pi\alpha \frac{1}{m_e T_e^2} e_{\nu_e}^2. \tag{55}$$

In reactor experiments the neutrino magnetic moment is searched by considering data with $T_e \ll E_\nu$. The ratio of the charge cross section (55) and the magnetic moment cross section in Eq. (20), for which we consider only the dominant part proportional to $1/T_e$, is given by

$$R = \frac{(d\sigma/dT_e)_{\mathrm{charge}}}{(d\sigma/dT_e)_{\mathrm{mag}}} \simeq \frac{2m_e}{T_e} \frac{\left(e_{\nu_e}/e\right)^2}{\left(\mu_{\nu_e}/\mu_{\mathrm{B}}\right)^2} \tag{56}$$

Considering an experiment which does not observe any effect of μ_{ν_e} and obtains a limit on μ_{ν_e}, it is possible to obtain, following [171], a bound on e_{ν_e} by demanding that the effect of e_{ν_e} is smaller than that of μ_{ν_e}, i.e. that $R \lesssim 1$:

$$e_{\nu_e}^2 \lesssim \frac{T_e}{2m_e} \left(\frac{\mu_{\nu_e}}{\mu_{\mathrm{B}}}\right)^2 e^2. \tag{57}$$

The last limit in Tab. 2 has been obtained from the 2012 results [50] of the GEMMA experiment, considering T_e at the experimental threshold of 2.8 keV.

Let us finally note that a strong limit on a generic neutrino electric charge e_ν can be obtained by considering the influence of millicharged neutrinos on the rotation of a magnetized star which is undergoing a core-collapse supernova explosion (the neutrino star turning mechanism, νST) [173]. During the supernova explosion, the escaping millicharged neutrinos move along curved orbits inside the rotating magnetized star and slow down the rotation of the star. This mechanism could prevent the generation of a rapidly rotating pulsar in the supernova explosion. Imposing that the frequency shift of a forming pulsar due to the neutrino star turning mechanism is less than a typical observed frequency of $0.1\,\mathrm{s}^{-1}$ and assuming a magnetic field of the order of $10^{14}\,\mathrm{G}$, the author of [173] obtained

$$|e_\nu| \lesssim 1.3 \times 10^{-19}\, e. \tag{58}$$

Note that this limit is much stronger than the astrophysical limits in Tab. 2.

Neutrino charge radius. The neutrino charge radius has an effect in the scattering of neutrinos with charged particles. The most useful process is the elastic scattering with electrons. Since in the ultrarelativistic limit the charge form factor conserves the neutrino helicity, a neutrino charge radius contributes to the weak interaction cross section $(d\sigma/dT_e)_{\mathrm{SM}}$ of ν_ℓ–e^- elastic scattering through the following shift of the vector coupling constant $g_V^{\nu_\ell}$ [42, 67, 177, 178]:

$$g_V^{\nu_\ell} \to g_V^{\nu_\ell} + \frac{2}{3} m_W^2 \langle r_{\nu_\ell}^2 \rangle \sin^2\theta_W. \tag{59}$$

Using this method, experiments which measure neutrino-electron elastic scattering can probe the neutrino charge radius. Some experimental results are listed in Tab. 3. In addition, the authors of [176] obtained the following 90% CL bounds on $\langle r_{\nu_\mu}^2 \rangle$ from a reanalysis of CHARM-II [175] and CCFR [179] data:

$$-0.52 \times 10^{-32} < \langle r_{\nu_\mu}^2 \rangle < 0.68 \times 10^{-32}\,\mathrm{cm}^2. \tag{60}$$

More recently, the authors of [180] obtained the following 90% CL bounds on $\langle r_{\nu_e}^2 \rangle$ from a combined fit of all available ν_e–e^- and $\bar{\nu}_e$–e^- data:

$$-0.26 \times 10^{-32} < \langle r_{\nu_e}^2 \rangle < 6.64 \times 10^{-32}\,\mathrm{cm}^2. \tag{61}$$

The single photon production process $e^+ + e^- \to \nu + \bar{\nu} + \gamma$ has been used to get bounds on the effective ν_τ charge radius, assuming a negligible contribution of the ν_e and ν_μ charge radii [176, 181, 182]. For Dirac neutrinos, the authors of [176] obtained

$$-5.6 \times 10^{-32} < \langle r_{\nu_\tau}^2 \rangle < 6.2 \times 10^{-32}\,\mathrm{cm}^2. \tag{62}$$

Limit	Method	Reference
$\lvert e_{\nu_\tau}\rvert \lesssim 3\times10^{-4}\,e$	SLAC e^- beam dump	[168]
$\lvert e_{\nu_\tau}\rvert \lesssim 4\times10^{-4}\,e$	BEBC beam dump	[169]
$\lvert e_{\nu}\rvert \lesssim 6\times10^{-14}\,e$	Solar cooling (plasmon decay)	[163]
$\lvert e_{\nu}\rvert \lesssim 2\times10^{-14}\,e$	Red giant cooling (plasmon decay)	[163]
$\lvert e_{\nu_e}\rvert \lesssim 3\times10^{-21}\,e$	Neutrality of matter	[163]
$\lvert e_{\nu_e}\rvert \lesssim 3.7\times10^{-12}\,e$	Nuclear reactor	[170]
$\lvert e_{\nu_e}\rvert \lesssim 1.5\times10^{-12}\,e$	Nuclear reactor	[171]

Table 2 Approximate limits for different neutrino effective charges. The limits on e_ν apply to all flavors.

Method	Experiment	Limit [cm^2]	CL	Reference
Reactor $\bar\nu_e$-e^-	Krasnoyarsk	$\lvert\langle r^2_{\nu_e}\rangle\rvert < 7.3\times10^{-32}$	90%	[132]
	TEXONO	$-4.2\times10^{-32} < \langle r^2_{\nu_e}\rangle < 6.6\times10^{-32}$	90%	[174]
Accelerator ν_e-e^-	LAMPF	$-7.12\times10^{-32} < \langle r^2_{\nu_e}\rangle < 10.88\times10^{-32}$	90%	[136]
	LSND	$-5.94\times10^{-32} < \langle r^2_{\nu_e}\rangle < 8.28\times10^{-32}$	90%	[138]
Accelerator ν_μ-e^-	BNL-E734	$-4.22\times10^{-32} < \langle r^2_{\nu_\mu}\rangle < 0.48\times10^{-32}$	90%	[137]
	CHARM-II	$\lvert\langle r^2_{\nu_\mu}\rangle\rvert < 1.2\times10^{-32}$	90%	[175]

Table 3 Experimental limits for the electron neutrino charge radius. In the TEXONO, LAMPF, LSND, BNL-E734, and CHARM-II cases, the published limits are half, because they use a convention which differs by a factor of 2 (see also Ref. [176]).

Comparing the theoretical Standard Model values with the experimental limits in Tab. 3 and those in Eqs. (60)–(62), one can see that they differ at most by one order of magnitude. Therefore, one may expect that the experimental accuracy will soon reach the value needed to probe the Standard Model predictions for the neutrino charge radii. This will be an important test of the Standard Model calculation of the neutrino charge radii. If the experimental value of a neutrino charge radius is found to be different from the Standard Model prediction it will be necessary to clarify the precision of the theoretical calculation in order to understand if the difference is due to new physics beyond the Standard Model.

The neutrino charge radius has also some impact on astrophysical phenomena and on cosmology. The limits on the cooling of the Sun and white dwarfs due to the plasmon decay process discussed in the previous Section induced by a neutrino charge radius led the authors of [183] to estimate the respective limits $\lvert\langle r^2_\nu\rangle\rvert \lesssim 10^{-28}\,\mathrm{cm}^2$ and $\lvert\langle r^2_\nu\rangle\rvert \lesssim 10^{-30}\,\mathrm{cm}^2$ for all neutrino flavors. From the cooling of red giants the authors of [181] inferred the limit $\lvert\langle r^2_\nu\rangle\rvert \lesssim 4\times10^{-31}\,\mathrm{cm}^2$.

If neutrinos are Dirac particles, e^+–e^- annihilations can produce right-handed neutrino-antineutrino pairs through the coupling induced by a neutrino charge radius. This process would affect primordial Big-Bang Nucleosynthesis and the energy release of a core-collapse supernova. From the measured ^{4}He yield in primordial Big-Bang Nucleosynthesis the authors of [184] obtained

$$\lvert\langle r^2_\nu\rangle\rvert \lesssim 7\times10^{-33}\,\mathrm{cm}^2, \tag{63}$$

and from SN 1987A data the authors of [185] obtained

$$\langle r^2_\nu\rangle \lesssim 2\times10^{-33}\,\mathrm{cm}^2, \tag{64}$$

for all neutrino flavors.

5 Future astrophysical probes of electromagnetic neutrinos

Solar neutrinos. The precision measurements of low-energy neutrinos from the Sun in the ongoing and forthcoming solar neutrino experiments will not only provide us with more accurate values of neutrino oscillation parameters [186], but also offer a precious opportunity to test the Mikheyev-Smirnov-Wolfenstein (MSW) matter effect [187, 188] and to probe the solar properties, such as the core metallicity (by measuring the CNO neutrino flux) and the total luminosity (through determining the pp neutrino flux). Furthermore, the observations of solar neutrinos in the future water-Cherenkov detector Hyper-Kamiokande [189] and liquid-scintillator detectors SNO+ [190], JUNO [191], RENO50 [192] and LENA [193] will greatly improve current knowledge about the electromagnetic properties of neutrinos.

Besides reactor antineutrino experiments, the neutrino-electron elastic scattering of low-energy solar neutrinos can also be used to measure the neutrino magnetic properties. The contribution of the neutrino magnetic dipole moment to the elastic ν_e-e^- cross section becomes more predominant as the electron kinetic energy T_e decreases since it is inversely proportional to T_e at low energy. Therefore, the measurements of solar neutrinos in the ^{8}B [130], ^{7}Be [131] and pp [194] processes may provide us excellent opportunities to constrain the neutrino magnetic dipole moment. As already reported in Table 1, the current upper limits at 90% C.L. obtained from the measurements of ^{8}B and ^{7}Be neutrinos are $1.1\times10^{-10}\mu_{\rm B}$ [130] and $5.4\times10^{-11}\mu_{\rm B}$ [131], respectively. Note that these are limits on effective magnetic moments which are different combinations of the magnetic dipole moments of massive neutrinos, as discussed at the beginning of Section 4.

In future, large liquid-scintillator detectors will improve the precision of low-energy solar neutrino measurements, and can give better limits on the magnetic dipole moment. There will be a liquid-scintillator detector with a 20 kiloton target mass and a high energy resolution of $3\%/\sqrt{E/\mathrm{MeV}}$ at JUNO, and the LENA detector will be 2.5 times larger. In consequence, JUNO [191] (LENA [193]) will register about four thousand (ten thousand) ^{7}Be elastic ν_e-e^- events per day in its detectable window above 250 keV, which means that the statistical uncertainties can be negligible after years of data-taking. Therefore, the achievable limit on the neutrino magnetic dipole moment mainly depends on the systematics, and in particular on the radioactive and cosmogenic backgrounds.

Another interesting solar neutrino process due to neutrino magnetic properties is the spin-flavor precession mechanism [38]. As discussed in Section 3, besides the standard MSW resonant transition, there might be interesting transitions between the left-handed and right-handed components of solar neutrinos in the presence of the solar magnetic field. In the case of Dirac neutrinos, the additional transition happens between the active and sterile neutrino states and can be a sub-leading effect in neutrino oscillation probabilities. More interestingly, in the case of Majorana neutrinos, right-handed neutrinos of the electron flavor produced in the spin-flavor precession can be detected with the inverse beta decay reaction, which can significantly reduce the singles background using the coincidence of prompt and delayed signals of the reaction. The recent measurement from Borexino [195] constrains the transition probability to be smaller than 1.3×10^{-4} (90% C.L.), which corresponds to an upper limit of $10^{-12}\mu_{\rm B} - 10^{-8}\mu_{\rm B}$ for the neutrino magnetic dipole moment. Future liquid-scintillator detectors (e.g. JUNO, RENO50 and LENA) are 1-2 orders of magnitude larger than Borexino and may improve the transition probability limits by one order of magnitude. This observation could be free of the reactor antineutrino background when one concentrates on the energy region larger than 10 MeV.

Supernova neutrinos. As is well known, the electromagnetic dipole interaction of massive neutrinos couples left-handed neutrinos to the right-handed ones. If neutrinos are Dirac particles, right-handed neutrino states are sterile and can be copiously produced in the supernova core, where large magnetic fields may exist. While the left-handed neutrinos are trapped inside the supernova core and come out by diffusion, the sterile ones can freely escape from the core immediately after production. Since the energy loss caused by right-handed neutrinos should not shorten significantly the duration of the neutrino signal, which has been observed by the Kamiokande-II, IMB and Baksan experiments to be about ten seconds, one can obtain the restrictive limit on the neutrino magnetic dipole moment $\mu_\nu \lesssim 3\times10^{-12}\mu_{\rm B}$ [163]. However, this bound applies only to massive Dirac neutrinos, since the right-handed states of Majorana neutrinos interact as Standard Model antineutrinos and do not induce any extra energy loss because they are trapped in the core.

Although it was pointed out long time ago that the neutrino-neutrino refraction in the supernova environment may be very important for neutrino flavor conversions, the nonlinear evolution of neutrino flavors has recently been found to dramatically change neutrino energy spectra [196]. Depending on the initial neutrino fluxes and energy spectra, a complete swap between neutrino spectra of electron and non-electron flavors can take place in the whole or a finite energy range, as a direct consequence of collective neutrino oscillations. The impact of

nonzero transition magnetic moments for massive Majorana neutrinos on collective neutrino oscillations has been explored in Ref. [197, 198]. For a magnetic field of 10^{12} G and $\mu_\nu \approx 10^{-22}\mu_B$, which is just two orders of magnitude larger than the Standard-Model prediction corresponding to neutrino masses of the order of 0.1 eV, the pattern of spectral splits of supernova neutrinos may be observed in future experiments.

For a future galactic supernova, a number of large water-Cherenkov (Super-Kamiokande [199] and Hyper-Kamiokande), scintillator (JUNO, RENO50 and LENA) and liquid-argon (DUNE [200]) detectors will be able to perform a high-statistics measurement of galactic supernova neutrinos. In the case of a galactic supernova at a typical distance of 10 kpc, the JUNO detector will record about 5000 inverse beta-decay events, implying a precise determination of $\overline{\nu}_e$ energy spectrum. In addition, the charged-current interaction $\nu_e + {}^{12}\mathrm{C} \to e^- + {}^{12}\mathrm{N}$ contributes to a few hundred events, which together with the elastic ν_e-e^- scattering leads to a possible measurement of ν_e energy spectrum. Finally, the number of elastic neutrino-proton scattering events reaches two thousand, since JUNO is expected to achieve a threshold around 0.1 or 0.2 MeV for the proton recoil energy. Combining these measurements with the information from the water-Cherenkov and liquid-argon detectors, we hope to pin down the neutrino energy spectra with reasonable accuracy. The identification of the spectral splits will allow us to probe values of the neutrino magnetic moments which are extremely small and impossible to detect in other terrestrial experiments. Unfortunately, the experimental determination of the neutrino magnetic moments will be complicated by the distorsions of the neutrino spectra induced by the ordinary Mikheyev-Smirnov-Wolfenstein effects in the supernova envelope and by the Earth matter effects.

Cosmological observations. The early Universe is another place where neutrinos can be in thermal equilibrium and play a very important role. The phase transitions in the early Universe can have generated primordial magnetic fields, which populated the right-handed neutrinos if neutrinos are Dirac particles and have finite magnetic dipole moments. If the magnetic dipole interaction rate of neutrinos is larger than the Hubble expansion rate during the epoch of primordial nucleosynthesis, the right-handed neutrinos are in thermal equilibrium and contribute to the effective number of neutrino species by $\Delta N_\nu = 3$, which will modify the correct predictions of the standard BBN theory for the abundance of light nuclear elements. As shown in Refs. [201,202], the requirement for the magnetic dipole interaction rate to be smaller than the Hubble expansion rate at $T = 200$ MeV, when the QCD phase transition occurs, leads to an upper bound on the neutrino magnetic dipole moment. For a primordial magnetic field $B_0 = 10^{-14}$ G and the size of magnetic field domain $\lambda = 1$ Mpc, one can derive a tight bound $\mu_\nu < 10^{-16}\ \mu_B$, which is several orders of magnitude below current experimental limits [202].

6 Summary and prospects

In this review we outlined some aspects of the physics of electromagnetic neutrinos. No experimental evidence in favor of neutrino electromagnetic interactions has been obtained so far. All the neutrino electromagnetic characteristics have rather stringent upper bounds, which are due to laboratory experiments or from astrophysical observations.

The most accessible neutrino electromagnetic property may be the charge radius, for which the Standard Model gives a value which is only about one order of magnitude smaller than the experimental upper bounds. A measurement of a neutrino charge radius at the level predicted by the Standard Model would be another spectacular confirmation of the Standard Model, after the recent discovery of the Higgs boson (see [203]). However, such a measurement would not give information on new physics beyond the Standard Model unless the measured value is shown to be incompatible with the Standard Model value in a high-precision experiment.

The strongest current efforts to probe the physics beyond the Standard Model by measuring neutrino electromagnetic properties is the search for a neutrino magnetic moment effect in reactor $\bar{\nu}_e$-e^- scattering experiments. The current upper bounds reviewed in Section 4 are more than eight orders of magnitude larger than the prediction discussed in Section 2 of the Dirac neutrino magnetic moments in the minimal extension of the Standard Model with right-handed neutrinos. Hence, a discovery of a neutrino magnetic moment effect in reactor $\bar{\nu}_e$-e^- scattering experiments would be a very exciting evidence of non-minimal new physics beyond the Standard Model.

In particular, the GEMMA-II collaboration expects to reach around the year 2017 a sensitivity to $\mu_{\nu_e} \approx 1 \times 10^{-11}\mu_B$ in a new series of measurements at the Kalinin Nuclear Power Plant with a doubled neutrino flux obtained by reducing the distance between the reactor and the detector from 13.9 m to 10 m and by lowering the energy threshold from 2.8 keV to 1.5 keV [50,204]. The corresponding sensitivity to the neutrino electric millicharge will reach the level of $|e_{\nu_e}| \approx 3.7 \times 10^{-13}\, e$ [171].

There is also a GEMMA-III project[6] to further lower the energy threshold to about 350 eV, which may allow the experimental collaboration to reach a sensitivity of $\mu_{\nu_e} \approx 9 \times 10^{-12} \mu_B$. The corresponding sensitivity to neutrino millicharge will be $|e_{\nu_e}| \approx 1.8 \times 10^{-13}\, e$ [171].

An interesting possibility for exploring very small values of μ_{ν_e} in $\bar{\nu}_e$-e^- scattering experiments has been proposed in Ref. [205] on the basis of the observation [206] that "dynamical zeros" induced by a destructive interference between the left-handed and right-handed chiral couplings of the electron in the charged and neutral current amplitudes appear in the Standard Model contribution to the scattering cross section. It may be possible to enhance the sensitivity of an experiment to μ_{ν_e} by selecting recoil electrons contained in a forward narrow cone corresponding to a dynamical zero (see Eq. (14)).

In the future, experimental searches of neutrino electromagnetic properties may be performed also with new neutrino sources, as a tritium source [207], a low-energy beta-beam [207, 208], a stopped-pion neutrino source [83], or a neutrino factory [208]. Recently the authors of Ref. [209] proposed to improve the existing limit on the electron neutrino magnetic moment with a megacurie ^{51}Cr neutrino source and a large liquid Xe detector.

Neutrino electromagnetic interactions could have important effects in astrophysical environments and in the evolution of the Universe and the current rapid advances of astrophysical and cosmological observations may lead soon to the very exciting discovery of nonstandard neutrino electromagnetic properties. In particular, future high-precision observations of supernova neutrino fluxes may reveal the effects of collective spin-flavor oscillations due to Majorana transition magnetic moments as small as $10^{-21}\, \mu_B$ [197, 198].

Let us finally emphasize the importance to pursue the experimental and theoretical studies of electromagnetic neutrinos, which could open a door to new physics beyond the Standard Model.

Acknowledgements. This work was supported in part by the joint project of the Russian Foundation for Basic Research (RFBR) under Grant No. 15-52-53112 and National Natural Science Foundation of China (NSFC) under Grant No. 11511130016. The work of C. Giunti was partially supported by the PRIN 2012 research grant 2012CPPYP7. The work of K. A. Kouzakov, A. V. Lokhov, and A. I. Studenikin was also supported in part by the RFBR under Grant No. 14-22-03043-ofi-m, and that of Yu-Feng Li and Shun Zhou by the NSFC under Grant Nos. 11135009, 11305193, by the Innovation Program of the Institute of High Energy Physics under Grant No. Y4515570U1, and by the CAS Center for Excellence in Particle Physics (CCEPP). K. A. Kouzakov also acknowledges support from the RFBR under Grant No. 14-01-00420-a.

Key words. Neutrino, Beyond Standard Model, Neutrino electromagnetic properties.

[6] Victor Brudanin and Vyacheslav Egorov, private communication.

References

[1] W. Pauli, Camb. Monogr. Part. Phys. Nucl. Phys. Cosmol. **1**, 1 (1991).
[2] W. Marciano and A. Sanda, Phys. Lett. B **67**, 303 (1977).
[3] B. W. Lee and R. E. Shrock, Phys. Rev. D **16**, 1444 (1977).
[4] K. Fujikawa and R. Shrock, Phys. Rev. Lett. **45**, 963 (1980).
[5] S. Petcov, Sov. J. Nucl. Phys. **25**, 340 (1977).
[6] P. B. Pal and L. Wolfenstein, Phys. Rev. D **25**, 766 (1982).
[7] R. E. Shrock, Nucl. Phys. B **206**, 359 (1982).
[8] S. M. Bilenky and S. Petcov, Rev. Mod. Phys. **59**, 671 (1987).
[9] F. Reines, C. Cowan, F. Harrison, A. McGuire, and H. Kruse, Phys. Rev. **117**, 159 (1960).
[10] L. Landau, Nucl. Phys. **3**, 127 (1957).
[11] T. Lee and C. N. Yang, Phys. Rev. **105**, 1671 (1957).
[12] A. Salam, Nuovo Cim. **5**, 299 (1957).
[13] L. Radicati and B. Touschek, Nuovo Cim. **5**, 1693 (1957).
[14] K. Case, Phys. Rev. **107**, 307 (1957).
[15] J. A. Mclennan, Phys. Rev. **106**, 821 (1957).
[16] S. Glashow, Nucl. Phys. **22**, 579 (1961).
[17] S. Weinberg, Phys. Rev. Lett. **19**, 1264 (1967).
[18] A. Salam, Conf. Proc. **C680519**, 367 (1968).
[19] C. Giunti and C. W. Kim, Fundamentals of Neutrino Physics and Astrophysics (Oxford University Press, 2007).
[20] S. Bilenky, Lect. Notes Phys. **817**, 1 (2010).
[21] Z. Z. Xing and S. Zhou, Neutrinos in Particle Physics, Astronomy and Cosmology (Zhejiang University Press, 2011).
[22] M. Gonzalez-Garcia, M. Maltoni, J. Salvado, and T. Schwetz, JHEP **1212**, 123 (2012).
[23] G. Bellini, L. Ludhova, G. Ranucci, and F. Villante, Adv. High Energy Phys. **2014**, 191960 (2014).
[24] J. Beringer et al., Phys. Rev. D **86**, 010001 (2012).
[25] B. Pontecorvo, Sov. Phys. JETP **6**, 429 (1957).
[26] B. Pontecorvo, Sov. Phys. JETP **7**, 172 (1958).
[27] Z. Maki, M. Nakagawa, and S. Sakata, Prog. Theor. Phys. **28**, 870–880 (1962).
[28] B. Pontecorvo, Sov. Phys. JETP **26**(May), 984 (1968).

[29] P. Ramond, Journeys beyond the Standard Model (Cambridge, Mass.: Perseus Books, 1999).
[30] R. N. Mohapatra and P. B. Pal, Massive Neutrinos in Physics and Astrophysics (World Scientific, 2004), Third Edition, Lecture Notes in Physics, Vol. 72.
[31] B. Kayser, Phys. Rev. D **26**, 1662 (1982).
[32] R. Foot, H. Lew, and R. Volkas, J. Phys. G **19**, 361 (1993).
[33] W. A. Bardeen, R. Gastmans, and B. Lautrup Nucl. Phys. B **46**, 319 (1972).
[34] L. Cabral-Rosetti, J. Bernabeu, J. Vidal, and A. Zepeda, Eur. Phys. J. C **12**, 633 (2000).
[35] M. Dvornikov and A. Studenikin, Phys. Rev. D **69**, 073001 (2004).
[36] M. S. Dvornikov and A. I. Studenikin, J. Exp. Theor. Phys. **99**, 254 (2004).
[37] S. Davidson, S. Hannestad, and G. Raffelt JHEP **0005**, 003 (2000).
[38] C. Giunti and A. Studenikin, Rev. Mod. Phys. **87**, 531 (2015).
[39] S. Lee, Phys. Rev. D **6**, 1701 (1972).
[40] J. Lucio, A. Rosado, and A. Zepeda, Phys. Rev. D **29**, 1539 (1984).
[41] J. Lucio, A. Rosado, and A. Zepeda, Phys. Rev. D **31**, 1091 (1985).
[42] G. Degrassi, A. Sirlin, and W. Marciano Phys. Rev. D **39**, 287 (1989).
[43] J. Bernabeu, L. G. Cabral-Rosetti, J. Papavassiliou, and J. Vidal, Phys. Rev. D **62**, 113012 (2000).
[44] J. Bernabeu, J. Papavassiliou, and J. Vidal Phys. Rev. Lett. **89**, 101802 (2002).
[45] J. Bernabeu, J. Papavassiliou, and J. Vidal Nucl. Phys. B **680**, 450 (2004).
[46] K. Fujikawa and R. Shrock, arXiv:0303188 (2003).
[47] K. Fujikawa and R. Shrock, Phys. Rev. D **69**, 013007 (2004).
[48] J. Papavassiliou, J. Bernabeu, D. Binosi, and J. Vidal, Eur. Phys. J. C **33**, S865 (2004).
[49] J. Bernabeu, J. Papavassiliou, and D. Binosi Nucl. Phys. B **716**, 352 (2005).
[50] A. Beda, V. Brudanin, V. Egorov, D. Medvedev, V. Pogosov et al., Adv. High Energy Phys. **2012**, 350150 (2012).
[51] G. Raffelt, Phys. Rev. Lett. **64**, 2856 (1990).
[52] N. Viaux et al., Astron. Astrophys. **558**, A12 (2013).
[53] I. B. Zel'Dovich, Soviet Journal of Experimental and Theoretical Physics **6**, 1184 (1958).
[54] J. E. Kim, V. Mathur, and S. Okubo, Phys. Rev. D **9**, 3050 (1974).
[55] J. E. Kim, Phys. Rev. Lett. **41**, 360 (1978).
[56] D. A. Dicus, E. W. Kolb, H. Lubatti, and V. L. Teplitz, Phys. Rev. D **19**, 1522 (1979).
[57] A. Rosado and A. Zepeda, Phys.Rev. D **26**, 2517 (1982).
[58] H. Wong and H. B. Li, Mod. Phys. Lett. A **20**, 1103 (2005).
[59] A. Beda et al., Phys. Atom. Nucl. **70**, 1873 (2007).
[60] R. Mohapatra, S. P. Ng, and H. B. Yu, Phys. Rev. D **70**, 057301 (2004).
[61] J. Carlson and J. Oppenheimer, Phys. Rev. **41**, 763–792 (1932).
[62] H. Bethe, Math. Proc. Cambridge Philos. Soc. **31**, 108 (1935).
[63] A. V. Kyuldjiev, Nucl. Phys. B **243**, 387 (1984).
[64] G. Domogatsky and D. Nadezhin, Yad. Fiz. **12**, 1233 (1970).
[65] C. Cowan, F. Reines, and F. Harrison, Phys. Rev. **96**, 1294 (1954).
[66] C. Cowan and F. Reines, Phys. Rev. **107**, 528 (1957).
[67] P. Vogel and J. Engel, Phys. Rev. D **39**, 3378 (1989).
[68] W. Grimus and P. Stockinger, Phys. Rev. D **57**, 1762 (1998).
[69] K. A. Kouzakov and A. I. Studenikin, Phys. Lett. B **696**, 252 (2011).
[70] K. A. Kouzakov and A. I. Studenikin, Nucl. Phys. Proc. Suppl. **217**, 353 (2011).
[71] K. Kouzakov, A. Studenikin, and M. Voloshin JETP Lett. **93**, 623 (2011).
[72] K. A. Kouzakov, A. I. Studenikin, and M. B. Voloshin, Phys. Rev. D **83**, 113001 (2011).
[73] K. A. Kouzakov, A. I. Studenikin, and M. B. Voloshin, Nucl. Phys. Proc. Suppl. **229-232**, 496 (2012).
[74] V. Kopeikin, L. Mikaelyan, V. Sinev, and S. Fayans, Phys. At. Nucl. **60**, 1859 (1997).
[75] A. Balantekin, AIP Conf. Proc. **847**, 128 (2006).
[76] C. Giunti and A. Studenikin, Phys. Atom. Nucl. **72**, 2089 (2009).
[77] C. Broggini, C. Giunti, and A. Studenikin Adv. High Energy Phys. **2012**, 459526 (2012).
[78] D. Z. Freedman, Phys. Rev. D **9**, 1389 (1974).
[79] H. T. Wong, Int. J. Mod. Phys. D **20**, 1463 (2011).
[80] H. Li et al., Phys. Rev. Lett. **110**(26), 261301 (2013).
[81] H. Li et al., Astropart. Phys. **56**, 1 (2014).
[82] A. Drukier and L. Stodolsky, Phys. Rev. D **30**, 2295 (1984).
[83] K. Scholberg, Phys. Rev. D **73**, 033005 (2006).
[84] J. Barranco, O. Miranda, and T. Rashba, JHEP **0512**, 021 (2005).
[85] J. Barranco, O. Miranda, and T. Rashba, Phys. Rev. D **76**, 073008 (2007).
[86] S. Davidson, C. Pena-Garay, N. Rius, and A. Santamaria, JHEP **0303**, 011 (2003).
[87] R. Shrock, Phys. Rev. D **9**, 743 (1974).
[88] J. T. Goldman and G. J. Stephenson, Phys. Rev. D **16**, 2256 (1977).
[89] G. Zatsepin and A. Y. Smirnov, Yad. Fiz. **28**, 1569 (1978).
[90] D. A. Dicus, E. W. Kolb, and V. L. Teplitz Phys. Rev. Lett. **39**, 168 (1977).
[91] K. Sato and M. Kobayashi, Prog. Theor. Phys. **58**, 1775 (1977).
[92] F. Stecker, Phys. Rev. Lett. **45**, 1460 (1980).
[93] R. Kimble, S. Bowyer, and P. Jakobsen, Phys. Rev. Lett. **46**, 80 (1981).

[94] A. Melott and D. Sciama, Phys. Rev. Lett. **46**, 1369 (1981).
[95] A. De Rujula and S. Glashow, Phys. Rev. Lett. **45**, 942 (1980).
[96] J. C. D'Olivo, J. F. Nieves, and P. B. Pal Phys. Rev. Lett. **64**, 1088 (1990).
[97] S. Glashow, J. Iliopoulos, and L. Maiani Phys. Rev. D **2**, 1285 (1970).
[98] D. Grasso and V. Semikoz, Phys. Rev. D **60**, 053010 (1999).
[99] C. Giunti, C. Kim, and W. Lam, Phys. Rev. D **43**, 164 (1991).
[100] A. Lobanov and A. Studenikin, Phys. Lett. B **564**, 27 (2003).
[101] A. Studenikin and A. Ternov, Phys. Lett. B **608**, 107 (2005).
[102] A. Lobanov, Phys. Lett. B **619**, 136 (2005).
[103] A. Grigoriev, A. Studenikin, and A. Ternov Grav. Cosmol. **11**, 132 (2005).
[104] A. Sokolov and I. Ternov, Sov. Phys. Dokl. **8**, 1203 (1964).
[105] A. Grigoriev, A. Lokhov, A. Studenikin, and A. Ternov, Nuovo Cim. C **035N1**, 57 (2012).
[106] A. Grigoriev, A. Lokhov, A. Studenikin, and A. Ternov, Phys. Lett. B **718**, 512 (2012).
[107] A. Grigoriev, A. Lokhov, A. Studenikin, and A. Ternov, Nucl. Phys. Proc. Suppl. **229-232**, 447 (2012).
[108] A. Grigoriev, A. Lokhov, A. Studenikin, and A. Ternov, arXiv:1003.0630 (2010).
[109] A. I. Ternov and P. A. Eminov, Phys. Rev. D **87**, 113001 (2013).
[110] A. Cisneros, Astrophys. Space Sci. **10**, 87 (1971).
[111] M. B. Voloshin and M. I. Vysotsky, Sov. J. Nucl. Phys. **44**, 544 (1986).
[112] L. B. Okun, M. B. Voloshin, and M. I. Vysotsky, Sov. Phys. JETP **64**, 446 (1986).
[113] E. K. Akhmedov, Sov. J. Nucl. Phys. **48**, 382 (1988).
[114] C. S. Lim and W. J. Marciano, Phys. Rev. D **37**, 1368 (1988).
[115] E. K. Akhmedov and J. Pulido, Phys. Lett. B **553**, 7 (2003).
[116] B. C. Chauhan, J. Pulido, and E. Torrente-Lujan Phys. Rev. D **68**, 033015 (2003).
[117] O. G. Miranda, T. I. Rashba, A. I. Rez, and J. W. F. Valle, Phys. Rev. Lett. **93**, 051304 (2004).
[118] O. G. Miranda, T. I. Rashba, A. I. Rez, and J. W. F. Valle, Phys. Rev. D **70**, 113002 (2004).
[119] A. B. Balantekin and C. Volpe, Phys. Rev. D **72**, 033008 (2005).
[120] M. M. Guzzo, P. C. de Holanda, and O. L. G. Peres, Phys. Rev. D **72**, 073004 (2005).
[121] A. Friedland, arXiv:0505165 (2005).
[122] D. Yilmaz, arXiv:0810.1037 (2008)
[123] A. Borisov, V. C. Zhukovsky, A. Kurilin, and A. Ternov, Yad. Fiz. **41**, 743 (1985).
[124] S. Gavrilov and D. Gitman, Phys. Rev. D **87**, 125025 (2013).
[125] A. Studenikin, Phys. Atom. Nucl. **67**, 993 (2004).
[126] A. Egorov, A. Lobanov, and A. Studenikin Phys. Lett. B **491**, 137 (2000).
[127] A. Lobanov and A. Studenikin, Phys. Lett. B **515**, 94 (2001).
[128] A. Studenikin, arXiv:0407010 (2004).
[129] J. F. Beacom and P. Vogel, Phys. Rev. Lett. **83**, 5222 (1999).
[130] D. Liu et al., Phys. Rev. Lett. **93**, 021802 (2004).
[131] C. Arpesella et al., Phys. Rev. Lett. **101**, 091302 (2008).
[132] G. Vidyakin, V. Vyrodov, I. Gurevich, Y. Kozlov, V. Martemyanov et al., JETP Lett. **55**, 206 (1992).
[133] A. Derbin, A. Chernyi, L. Popeko, V. Muratova, G. Shishkina et al., JETP Lett. **57**, 768 (1993).
[134] Z. Daraktchieva et al., Phys. Lett. B **615**, 153 (2005).
[135] H. Wong et al., Phys. Rev. D **75**, 012001 (2007).
[136] R. Allen, H. Chen, P. Doe, R. Hausammann, W. Lee et al., Phys. Rev. D **47**, 11 (1993).
[137] L. Ahrens, S. Aronson, P. Connolly, B. Gibbard, M. Murtagh et al., Phys. Rev. D **D**, 3297 (1990).
[138] L. Auerbach et al., Phys. Rev. D **63**, 112001 (2001).
[139] R. Schwienhorst et al., Phys. Lett. B **513**, 23 (2001).
[140] F. Reines, H. Gurr, and H. Sobel, Phys. Rev. Lett. **37**, 315 (1976).
[141] H. T. Wong, H. B. Li, and S. T. Lin, Phys. Rev. Lett. **105**, 061801 (2010).
[142] M. Voloshin, Phys. Rev. Lett. **105**, 201801 (2010).
[143] J. W. Chen, H. C. Chi, K. N. Huang, C. P. Liu, H. T. Shiao et al., Phys. Lett. B **731**, 159 (2014).
[144] K. A. Kouzakov and A. I. Studenikin, Adv. High Energy Phys. **2014**, 569409 (2014).
[145] J. Barranco, A. Bolanos, E. Garces, O. Miranda, and T. Rashba, Int. J. Mod. Phys. A **27**, 1250147 (2012).
[146] K. J. Healey, A. A. Petrov, and D. Zhuridov Phys. Rev. D **87**, 117301 (2013).
[147] A. S. Joshipura and S. Mohanty, Phys. Rev. D **66**, 012003 (2002).
[148] W. Grimus, M. Maltoni, T. Schwetz, M. Tortola, and J. Valle, Nucl. Phys. B **648**, 376 (2003).
[149] M. Tortola, PoS **AHEP2003**, 022 (2003).
[150] H. Li et al., Phys. Rev. Lett. **90**, 131802 (2003).
[151] Z. Daraktchieva et al., Phys. Lett. B **564**, 190 (2003).
[152] A. Dar, Preprint-87-0178 (IAS, Princeton) (1987).
[153] S. Nussinov and Y. Rephaeli, Phys. Rev. D **36**, 2278 (1987).
[154] I. Goldman, Y. Aharonov, G. Alexander, and S. Nussinov, Phys. Rev. Lett. **60**, 1789 (1988).
[155] J. Lattimer and J. Cooperstein, Phys. Rev. Lett. **61**, 23 (1988).
[156] R. Barbieri and R. N. Mohapatra, Phys. Rev. Lett. **61**, 27 (1988).
[157] D. Notzold, Phys. Rev. D **38**, 1658 (1988).
[158] M. Voloshin, Phys. Lett. B **209**, 360 (1988).
[159] A. Ayala, J. C. D'Olivo, and M. Torres Phys. Rev. D **59**, 111901 (1999).

[160] A. Ayala, J. C. D'Olivo, and M. Torres Nucl. Phys. B **564**, 204 (2000).
[161] A. Balantekin, C. Volpe, and J. Welzel, JCAP **0709**, 016 (2007).
[162] G. Raffelt, Stars as Laboratories for Fundamental Physics: The Astrophysics of Neutrinos, Axions, and other Weakly Interacting Particles (University of Chicago Press, 1996).
[163] G. Raffelt, Phys. Rep. **320**, 319 (1999).
[164] G. Bressi et al., arXiv:1102.2766 (2011).
[165] J. Baumann, J. Kalus, R. Gahler, and W. Mampe, Phys. Rev. D **37**, 3107 (1988).
[166] M. Marinelli and G. Morpurgo, Phys. Lett. B **137**, 439 (1984).
[167] G. Barbiellini and G. Cocconi, Nature **329**, 21 (1987).
[168] S. Davidson, B. Campbell, and D. C. Bailey Phys. Rev. D **43**, 2314 (1991).
[169] K. Babu, T. M. Gould, and I. Rothstein Phys. Lett. B **321**, 140 (1994).
[170] S. Gninenko, N. Krasnikov, and A. Rubbia Phys. Rev. D **75**, 075014 (2007).
[171] A. Studenikin, Europhys. Lett. **107**, 21001 (2014).
[172] V. Berestetskii, E. Lifshitz, and L. Pitaevskii, Quantum Electrodynamics (Vol. 4 of Course of Theoretical Physics) (Pergamon, 1979).
[173] A. I. Studenikin and I. Tokarev, Nucl. Phys. B **884**, 396 (2014).
[174] M. Deniz et al., Phys. Rev. D **81**, 072001 (2010).
[175] P. Vilain et al., Phys. Lett. B **345**, 115 (1995).
[176] M. Hirsch, E. Nardi, and D. Restrepo, Phys. Rev. D **67**, 033005 (2003).
[177] A. Grau and J. Grifols, Phys. Lett. B **166**, 233 (1986).
[178] K. Hagiwara, S. Matsumoto, D. Haidt, and C. Kim, Z. Phys. C **64**, 559 (1994).
[179] K. S. McFarland et al., Eur. Phys. J. C **1**, 509 (1998).
[180] J. Barranco, O. Miranda, and T. Rashba, Phys. Lett. B **662**, 431 (2008).
[181] T. Altherr and P. Salati, Nucl. Phys. B **421**, 662 (1994).
[182] N. Tanimoto, I. Nakano, and M. Sakuda, Phys. Lett. B **478**, 1 (2000).
[183] A. Dolgov and Y. Zeldovich, Rev. Mod. Phys. **53**, 1 (1981).
[184] J. Grifols and E. Masso, Mod. Phys. Lett. A **2**, 205 (1987).
[185] J. Grifols and E. Masso, Phys. Rev. D **40**, 3819 (1989).
[186] K. Olive et al., Chin. Phys. C **38**, 090001 (2014).
[187] S. Mikheev and A. Y. Smirnov, Sov. J. Nucl. Phys. **42**, 913 (1985).
[188] L. Wolfenstein, Phys. Rev. D **17**, 2369 (1978).
[189] K. Abe et al., arXiv:1109.3262 (2011).
[190] C. Kraus and S. J. Peeters, Prog. Part. Nucl. Phys. **64**, 273 (2010).
[191] Y. F. Li, J. Cao, Y. Wang, and L. Zhan, Phys. Rev. D **88**, 013008 (2013).
[192] S. B. Kim, arXiv:1412.2199 (2014).
[193] M. Wurm et al., Astropart. Phys. **35**, 685 (2012).
[194] G. Bellini et al., Nature **512**(7515), 383 (2014).
[195] G. Bellini et al., Phys. Lett. B **696**, 191 (2011).
[196] H. Duan, G. M. Fuller, and Y. Z. Qian, Ann. Rev. Nucl. Part. Sci. **60**, 569 (2010).
[197] A. de Gouvea and S. Shalgar, JCAP **1210**, 027 (2012).
[198] A. de Gouvea and S. Shalgar, JCAP **1304**, 018 (2013).
[199] M. Ikeda et al., Astrophys. J. **669**, 519 (2007).
[200] C. Adams et al., arXiv:1307.7335 (2013).
[201] K. Enqvist, A. Rez, and V. Semikoz, Nucl. Phys. B **436**, 49 (1995).
[202] A. J. Long and T. Vachaspati, arXiv:1504.03319 (2015).
[203] J. Ellis, arXiv:1312.5672 (2013).
[204] A. Beda et al., Phys. Part. Nucl. Lett. **10**, 139 (2013).
[205] J. Bernabeu, J. Papavassiliou, and M. Passera, Phys. Lett. B **613**, 162 (2005).
[206] J. Segura, J. Bernabeu, F. Botella, and J. Penarrocha, Phys. Rev. D **49**, 1633 (1994).
[207] G. McLaughlin and C. Volpe, Phys. Lett. B **591**, 229 (2004).
[208] A. de Gouvea and J. Jenkins, Phys. Rev. D **74**, 033004 (2006).
[209] P. Coloma, P. Huber, and J. M. Link, JHEP **1411**, 042 (2014).